Journal of Neuroscience Methods 308 (2018) 286–293

Contents lists available at ScienceDirect

Journal of Neuroscience Methods

journal homepage: www.elsevier.com/locate/jneumeth

Derivation of phenotypically diverse neural culture from hESC by combining adherent and dissociation methods

Ye Liu[a,b,1], Ana Antonic[c,1], Xuan Yang[e], Nils Korte[f], Katherine Lim[g], Anna E. Michalska[g], Mirella Dottori[h], David W. Howells[d,*]

[a] Florey Institute of Neuroscience and Mental Health, 30 Royal Parade, The University of Melbourne, Victoria, 3010, Australia
[b] Department of Neurology, Fudan University, Huashan Hospital, Shanghai, 200040, China
[c] Department of Neuroscience, Central Clinical School, Monash University, The Alfred Centre, VIC, 3004, Australia
[d] School of Medicine, University of Tasmania, Hobart, Tasmania, 7001, Australia
[e] Institute for Geriatrics and Rehabilitation, Beijing Geriatric Hospital, Beijing, 100095, China
[f] Department of Neuroscience, Physiology and Pharmacology, University College London, Gower Street, London, WC1E6BT, UK
[g] Stem Cell Core Facility, Stem Cells Australia, The University of Melbourne, Victoria, 3010, Australia
[h] Illawarra Health and Medical Research Institute Centre for Molecular and Medical Bioscience Building 32, University of Wollongong, NSW, 2522 Australia

GRAPHICAL ABSTRACT

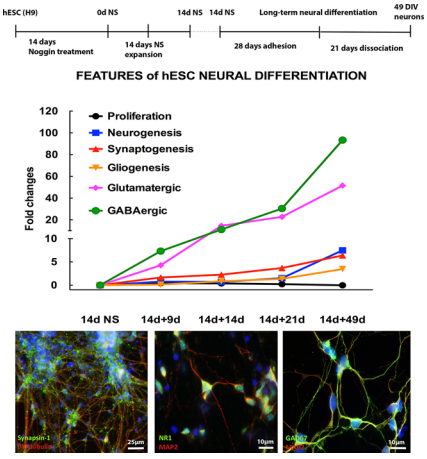

ARTICLE INFO

Keywords:
human embryonic stem cells
neuronal differentiation
neurochemical characterisation

ABSTRACT

Background: Differentiation of human embryonic stem cells (hESCs) into distinct neural lineages has been widely studied. However, preparation of mixed yet neurochemically mature populations, for the study of neurological diseases involving mixed cell types has received less attention.
New method: We combined two commonly used differentiation methods to provide robust and reproducible cultures in which a mixture of primarily GABAergic and Glutamatergic neurons was obtained. Detailed characterisation by immunocytochemistry (ICC) and quantitative real-time PCR (qPCR) assessed the neurochemical phenotype, and the maturation state of these neurons.
Results: We found that once neurospheres (NSs) had attached to the culture plates, proliferation of neural stem

* Corresponding author.
E-mail address: David.Howells@utas.edu.au (D.W. Howells).
[1] These authors contributed equally to this work.

https://doi.org/10.1016/j.jneumeth.2018.07.005
Received 13 January 2018; Received in revised form 5 July 2018; Accepted 5 July 2018
Available online 06 July 2018

cell was suppressed. Neuronal differentiation and synaptic development then occurred after 21 days *in vitro* (DIV). By 49DIV, there were large numbers of neurochemically and structurally mature neurons. The qPCR studies indicated that expression of GABAergic genes increased the most (93.3-fold increase), followed by glutamatergic (51-fold increase), along with smaller changes in expression of cholinergic (3-fold increase) and dopaminergic genes (6-fold increase), as well as a small change in glial cell marker expression (5-fold increase).
Comparison with existing method (s): Existing methods isolate hESC-derived neural progenitors for onward differentiation to mature neurons using either migration or dissociative paradigms. These give poor survival or yield. By combining these approaches, we obtain high yields of morphologically and neurochemically mature neurons. These can be maintained in culture for extended periods.
Conclusion: Our method provides a novel, effective and robust neural culture system with structurally and neurochemically mature cell populations and neural networks, suitable for studying a range of neurological diseases from a human perspective.

1. Introduction

Studying the mechanisms of neurological diseases *in vitro* still largely relies on rodent models (Hazzouri et al., 2014) or immortalised human cell lines (Alheim and Bartfai, 1998), which are unable to fully recapitulate the pathophysiology of human diseases, a deficiency which may contribute to translational failures in neuroscience (Landis et al., 2012). Since the first human embryonic stem cell (hESC) lines were derived from human blastocysts in 1998 (Thomson et al., 1998), their potential for regenerative medicine and mechanistic studies soon became recognised. The development of the first hESC-derived neural lineage cells in 2001 (Carpenter et al., 2001; Reubinoff et al., 2001) has proven extremely valuable for a wide range of studies on early human neurogenesis, modelling of neurological diseases and screening of neuro-pharmacological inventions. Importantly, the major neural cell types generated *in vitro* have recapitulated the key features and functions of the same cells in the adult brain (Dhara et al., 2008; Prajumwongs et al., 2016; Shinde et al., 2016).

Previous studies have focused on single transmitter phenotypes, such as the loss of dopaminergic neurons for modelling Parkinson's diseases (Datta et al., 2013) and the loss of GABAergic neurons for modelling Huntington's disease (Lee et al., 2009) or mixed population of dopaminergic and motor neurons (Chambers et al., 2009). Other studies have described maturation in terms of pan-neuronal markers (Lappalainen et al., 2010a) or not described maturation at all (Axell et al., 2009). In the case of most organoid cultures, the focus of the studies has been on the specificity of cortical layering (Pasca et al., 2015) rather than neurotransmitter phenotype. However, preparation of mixed neuronal populations with molecularly defined neurotransmitter characteristics has been less well studied. We have characterised the GABAergic, glutamatergic, cholinergic and dopaminergic profiles of our cultures.

Mixed neurotransmitter populations are important for the study of neurological diseases, which affect multiple cellular populations within large volume of tissue damage caused by insults such as stroke, neonatal hypoxia, traumatic brain injury or epilepsy. They are also likely to be important for the study of cell-cell interactions in these and other neurological diseases.

In the present study, we report a novel method to generate hESC-derived adherent cultures with structurally mature mixed neural populations in a simple and reproducible way. We also characterise the neurochemical specificity and the structural morphology by immunocytochemistry (ICC) and quantitative real-time PCR (qPCR).

2. Material and Methods

2.1. Neural induction by noggin treatment and neurosphere (NS) formation

H9 (WA09) hESC line was originally acquired from WiCell Research Institute, and regularly maintained in the Stem Cell Core Facility at the Florey Institute, Australia. Mycoplasma contamination was routinely tested. Initiation of neural specification was previously described (Dottori and Pera, 2007). Before use, the hESC colonies were ranked from 5 to 1. Colonies scoring 5 had the most ESC-like morphologically while colonies scoring 1 contained lots of cells with differentiated morphology (thicker, cyst-like with uneven surfaces). Only colonies scoring 5-4 were used, and from within these colonies the most undifferentiated areas (usually between the middle of the colony and the edge, presenting with a clean edge and tightly packed cells) were selected. In brief, undifferentiated portions of hESC colonies were mechanically cut into small pieces of approximately equal size, and plated onto mitotically inactivated mouse embryonic fibroblasts (MEFs) in hES

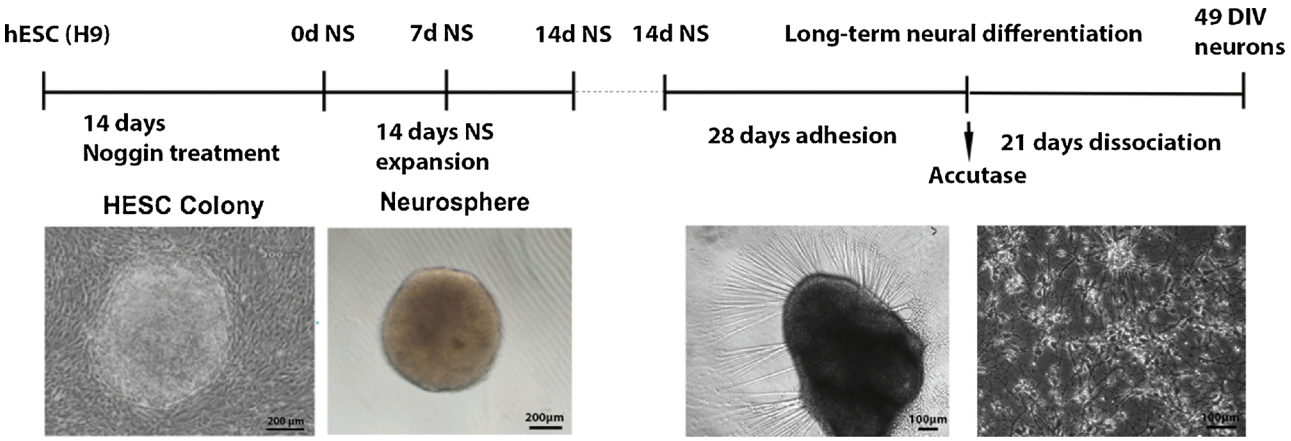

Fig. 1. Schematic timeline of human embryonic stem cells (hESCs) undergoing neural induction by noggin and differentiation over 49 days *in vitro* (DIV). hESCs were treated with noggin to induce neurosphere (NS) formation. After 14 days expansion, the 14-day NSs were plated down for 28 days, followed by another 21-day culture after dissociation to acquire 49DIV neurons.

medium (Supplementary material, Table 1) containing 500 ng/mL noggin (R&D systems, 6057-NG-100). The cells were cultured at 37∘C in 5% CO2 with 95% humidity for 14 days without passaging, and the medium was changed every other day. For the 0-day Noggin treated colonies, the colonies were full of rosettes, which were a sign of successful neural induction. To generate neurospheres (NSs), noggin treated colonies were cut using the tip of a 26-gauge needle on a grid so that the size of each sphere (approximately 500 x 500 µm) was much better controlled, and transferred to individual wells in a low adherent 96-well plate (Sigma Aldrich, CLS7007-24EA) containing Neurobasal Medium (NBM, components listed in Supplementary material, Table 2) supplemented with epidermal growth factor (EGF, Invitrogen, PHG0314, 20 ng/mL) and fibroblast growth factor (bFGF, Invitrogen, 13256029, 20 ng/mL). NSs were cultured in suspension for 14 days with the medium changed every second day (Fig. 1).

2.2. Differentiation and culture of hESC-derived neural cells for long term

Fourteen-day NSs were cut into smaller pieces under a dissection microscope (LEICA, IC80 HD) using the tip of a 26-gauge needle. Four to five pieces with similar size were placed into individual wells in a 24-well plate pre-coated with poly-d-lysine (PDL) and laminin (10 µg/mL, Sigma, P6407, Life Tech, 23017015). NS pieces were cultured in NBM without EGF and bFGF for 28 days and NBM was changed every two

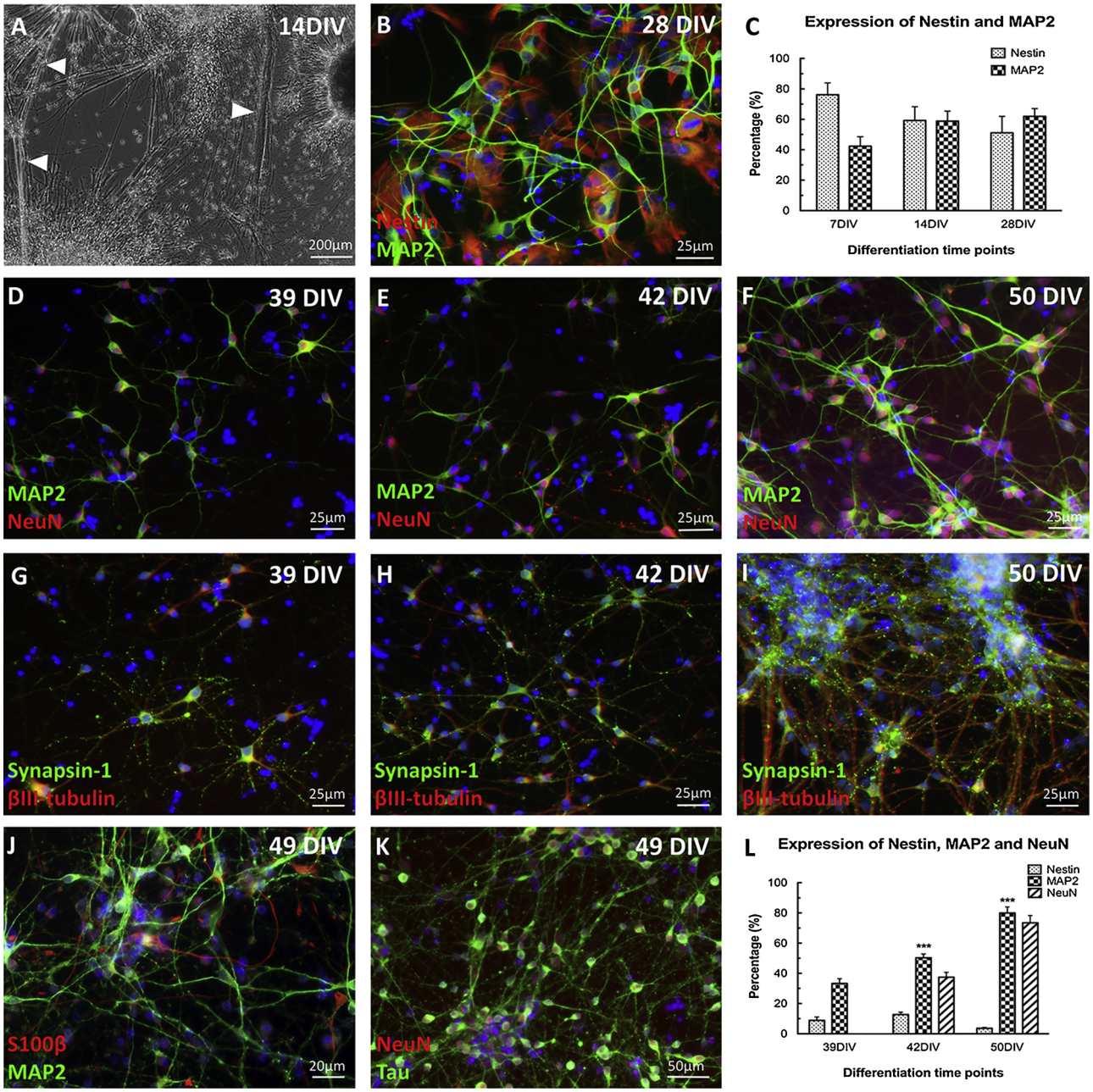

Fig. 2. Adhesion phases (A, B, C): 14-day NSs differentiated for 14DIV in phase contrast picture (A), or 28DIV with staining of Nestin and MAP2 at 28DIV (B). Quantitative immunocytochemistry (ICC) fluorescence measures of Nestin and MAP2 expression at 7, 14 and 21DIV (C). **Dissociation phases (D-L):** ICC staining with NeuN and MAP2 (D-F), and with βIII-tubulin and Synapsin1 (G-I) at 39, 42 and 50DIV. Staining with S100β and MAP2 at 49DIV (J). Staining with NeuN and Tau at 49DIV (K). Quantitative fluorescence measures of Nestin, MAP2 at 39, 42 and 50DIV and NeuN expression at 42 and 50DIV (L). Data is presented as mean ± SEM. Statistical significances are detected at $^{**}p < 0.01$, $^{***}p < 0.0001$ by one way-ANOVA with Bonferroni post-test comparing all columns across different time points.

days. Cell samples were collected on days 7, 9, 14 and 21 for subsequent analysis.

At 28 days, adherent cell cultures were treated with accutase (Thermo Fisher, A1110501, supplied as ready-to-use cell dissociation reagent) and incubated for 5 minutes at 37 °C to allow adherent cells to detach. Cell clumps were then collected and mechanically broken down by passing through a P1000 Gilson pipette until a homogenised cell suspension was achieved. Accutase was removed by dilution in an equal volume of NBM followed by centrifuged at 300 g for 4 minutes at room temperature. Cell pellets were then re-suspended in NBM, filtered through 40 µm cell strainers (BD, 352340), and plated onto PDL and laminin coated 35mm^2 dishes or coverslips (No 1, 13 mm round Menzel PK100, Grale Scientific, CS13100) at a density of 700,000 cells/dish. The cells were then incubated at 37 °C in 5% CO_2 with 95% humidity, and NBM was changed every second day until experiments terminated on days 39, 42, 49 and 50 (Fig. 1).

2.3. RNA extraction and quantitative real-time PCR (qPCR)

RNA was extracted for analysis from 14-day NSs and differentiated neural cells were harvested at 9, 14, 21 and 49 DIV. RNA extraction was performed using RNeasy Plus MINI Kits (Qiagen, cat. 74104) with DNA-free treatment (Qiagen, RNase-free DNase Set, 79254) following manufacturer's instructions. NanoDrop 2000 spectrophotometry (Thermo Fisher, ND-2000) was used to quantify the concentration and the purity of all samples. Only samples with an A260/A280 ratio between 1.9-2.1 were used. cDNA was synthesized following the recommended protocols from the SuperScript III First-Strand Synthesis SuperMix kit (Invitrogen; Cat. No: 18080-400) with RNA amount adjusted to 75 ng per cDNA reaction. Neural differentiation markers (SOX2, PAX6, MAP2, NESTIN, GAP43, SYN1, S100B, GFAP, OLIG2) were amplified using either in house-designed gene-specific primers or TaqMan primers (Supplementary material, Table 3). All qPCR reactions were performed in triplicates using an ABI 7900-HT system (Applied Biosystems) with no reverse transcriptase and primer controls included in each assay run. For all qPCR reactions, at least three independent experiments were conducted for each marker.

2.4. Immunocytochemistry (ICC)

Differentiated neural cells were fixed in 4% paraformaldehyde (PFA), and blocked in 10% foetal calf serum (FCS) before incubation with the appropriate concentration of primary antibodies (Supplementary material, Table 4) diluted in 3% FCS, and 0.3% Triton-x at 4 °C overnight. Secondary antibodies (Supplementary material, Table 5) were applied at a dilution of 1:500 (PBS containing 2% FCS) for 60 minutes at room temperature in the dark. A 1 mg/mL 4',6-diamidino-2-phenylindole (DAPI, Life Tech, 62248) stock solution was diluted in PBS (1:10, 000) before adding to the wells to stain for the nucleus. After 10 minutes, the DAPI solution was washed off twice with PBS before mounting the coverslips on glass slides with the anti-fade reagent (Molecular probes, P36930). The cells were visualised at 20x magnification using a Zeiss inverted fluorescence Microscope (Axio Observer 7).

2.5. MitoTracker staining

To stain mitochondria, the cell-permeant MitoTracker probe (ThermoFisher, M7512) was added to live cells in Neurobasal Medium at a concentration of 80 nM, and incubated for 30 minutes at 37 °C.

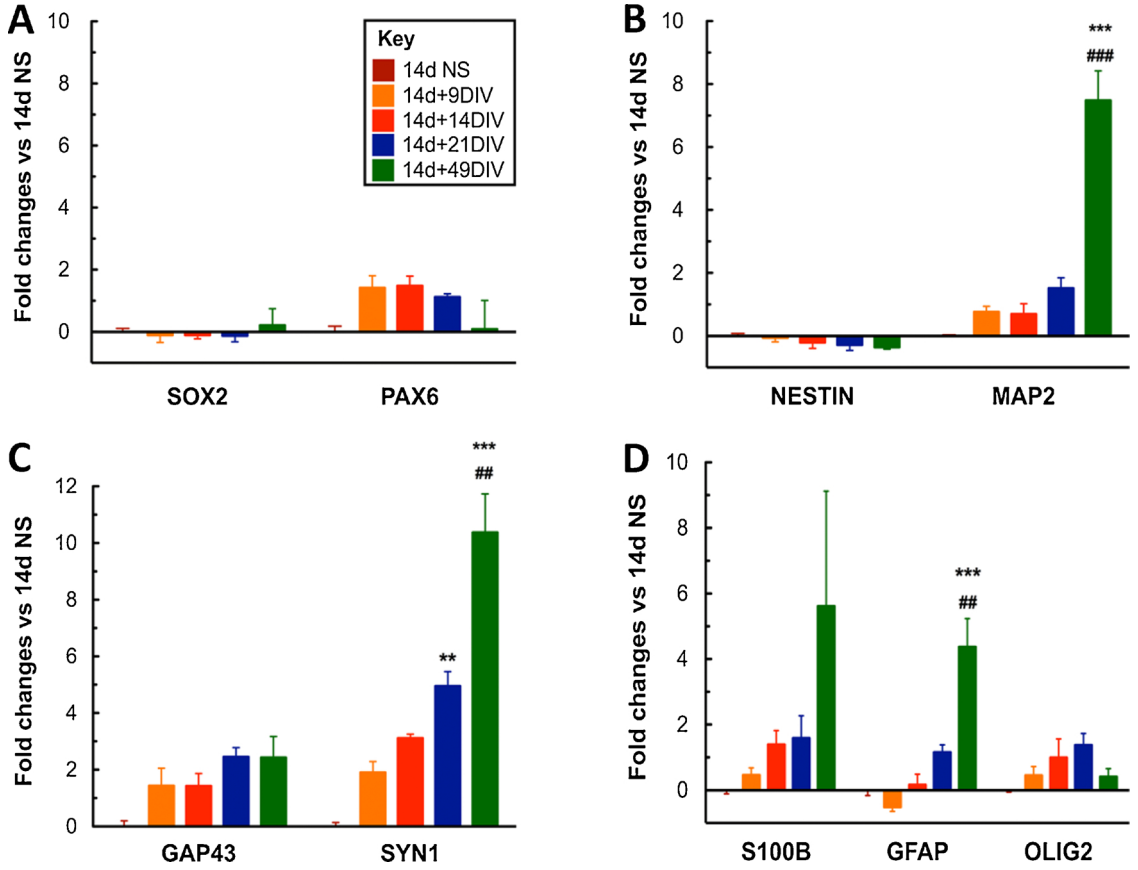

Fig. 3. Gene expression of pluripotency markers (A, B), synaptic markers (C) and glial markers (D) at different time points during hESC differentiation. Statistical significances are detected at *p < 0.05, **p < 0.01, ***p < 0.001 by one-way ANOVA. *, as compared to 14-day NS, #, as compared to the previous time points.

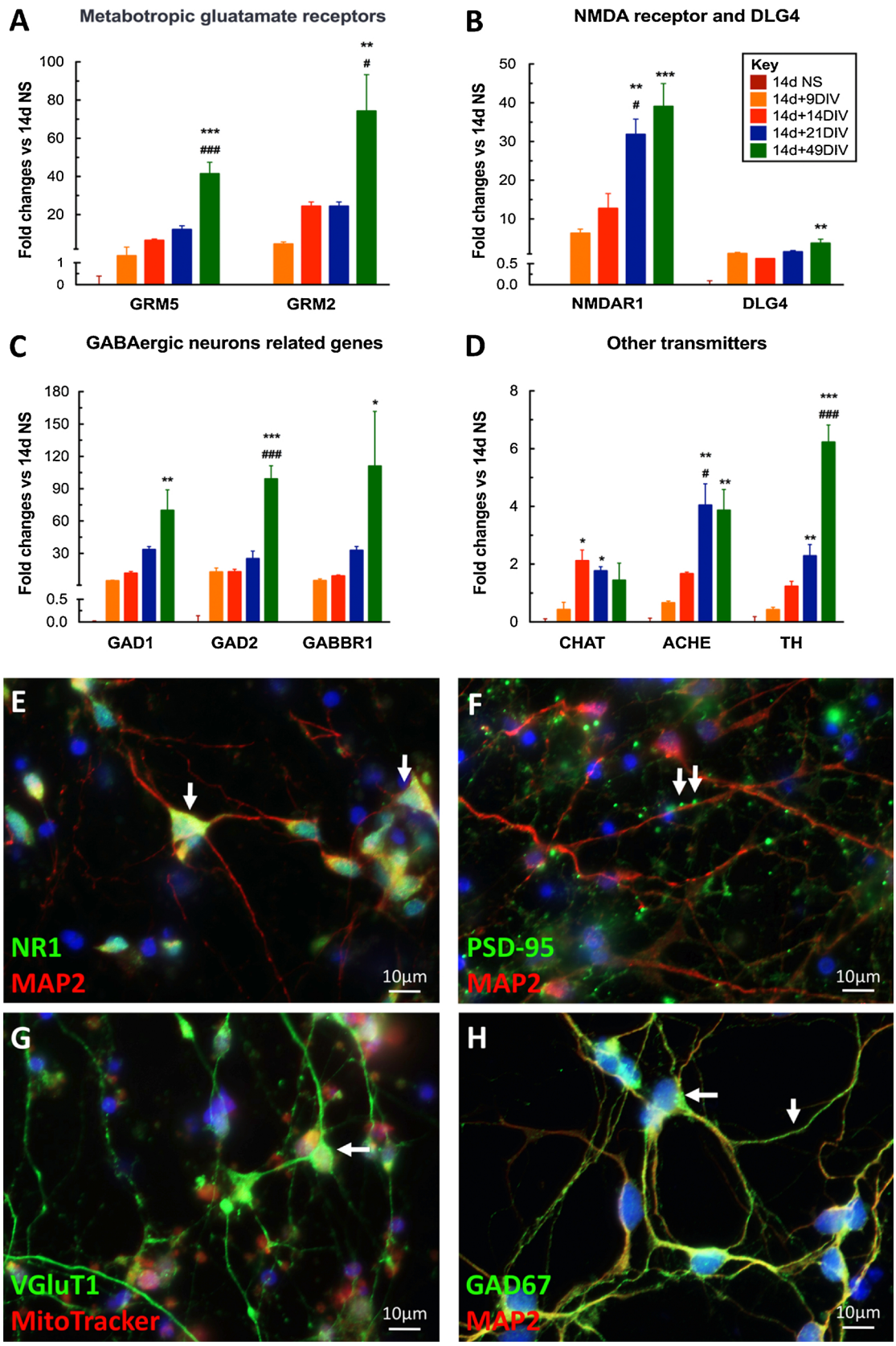

Fig. 4. Gene expression of glutamatergic neuronal markers (A, B), GABAergic neuronal markers (C) and other transmitter markers (D) at different time points during hESC differentiation. 14-day NSs differentiated for 49DIV, and stained for NR1 and MAP2 (E), PSD-95 and MAP2 (F), VGluT1 and MitoTracker (G) and GAD67 and MAP2 (H). Statistical significances are detected at *p < 0.05, **p < 0.01, ***p < 0.001 by One-way ANOVA. *, as compared to 14-day NS, #, as compared to the previous time points.

After three washes with PBS, the cells were fixed by immersion in 4% PFA before visualisation or further proceeding for ICC (see above).

2.6. Statistical analysis

Gene expression data (average of three replications) were acquired from ViiA7 Real-Time PCR system (ABI 7900-HT system), and relative fold change values were calculated using the ΔΔCt quantitation method (Schmittgen and Livak, 2008). GAPDH and ELF1 were used for normalisation and calibration of gene expression for each sample. All the fold changes were normalised to 14-day NS gene expression data. For immunocytochemistry, the total number of DAPI-positive nuclei and of immuno-positive cells was determined by manual counting using the standard features of Image J software (version 1.50i; NIH, Bethesda).

Each result depicted summarises the data from three independent experiments, each with multiple technical replicates (a minimum of two).

One-way analysis of variance (ANOVA) with Bonferroni post-hoc error correction was used to identify significant differences in gene and protein expression between time points. Data are presented as mean ± SEM. Statistical significance is detected at $p \leq 0.05$. At least three independent biological repeats were performed for each experiment.

3. Results

3.1. Neuronal maturation during hESC neural differentiation

When NS pieces were cultured (usually multiple pieces per well) (Fig. 2A, neurosphere piece 1/NS1, neurosphere piece2/NS2), they grew rapidly and sent out profuse neurites. As time in culture increased, the neurite mesh became more complex, often including what appeared to be large bundles of fibres between NSs (Fig. 2A, white arrows). During this period, expression of the neural stem cell marker Nestin showed a downward trend along with increasing differentiation, decreasing from 76.22 ± 7.77% at 7DIV to 55.11 ± 10.85% at 28DIV (Fig. 2B, C). By contrast, expression of the early neuronal marker MAP2 increased steadily from 42.33 ± 6.23% at 7DIV to 61.95 ± 5.16% at 28DIV (Fig. 2B, C). On average the 14d neurospheres had an area of 0.44 ± 0.1 mm2 (mean ± sem). For each experiment, all of the available neurospheres were pooled and dissociated, minimising the risk that an individual neurosphere with aberrant size or differentiation would unduly influence downstream culture.

Following dissociation, the number of Nestin positive cells declined further to around 10% of the total cell number and remained at this level until 50DIV. In contrast, MAP2 expression significantly increased from 33.34 ± 3.12% at 39DIV to 50.3 ± 2.52% ($p < 0.01$) at 42DIV and 80% ± 4.04% ($p < 0.001$) at 49DIV (Fig. 2L). Moreover, nearly 80% of the MAP2 positive cells present at 50DIV co-expressed the mature neuronal marker NeuN (Fig. 2F, L).

The synaptic marker Synapsin-1 was extensively co-expressed with βIII-tubulin in neuronal processes, and showed increased expression from 39DIV to 50DIV (Fig. 2G, H, I). At 49DIV, the cytoskeleton protein Tau was widely distributed both inside the cytoplasm and in neuronal processes. Additionally, the majority of Tau stained cells were also NeuN positive (Fig. 2K).

3.2. Characterization of neural cell lineage by ICC and qPCR

We next measured the mRNA levels for the early neural stem cell markers, neuronal and glial progenitor markers as well as markers of neurochemically mature neurons.

Expression of SOX2, a marker of neural stem cell/progenitor renewal, did not change significantly after the initiation of differentiation. Expression of PAX6, a transcription factor controlling regional patterning did not change significantly, although expression appeared slightly greater at 9DIV, 14DIV and 21DIV (Fig. 3A). Expression of NESTIN, a marker of commitment to a neural lineage, remained unchanged as more specialised differentiation continued. Conversely, expression of MAP2, a marker of neurite outgrowth increased significantly between 21 and 49DIV (7.5 ± 0.93 fold, $p < 0.001$) (Fig. 3B).

We also assessed expression of the synaptogenic markers GAP43 and SYN1. A trend towards increased expression of the growth cone marker GAP43 was seen after 21DIV and was then maintained to 49DIV (2.5 ± 0.75 fold). Expression of SYN1 became evident after 21DIV (5 ± 0.51 fold, $p < 0.01$), and steadily increased until 49DIV (10 ± 1.36 fold, $p < 0.001$) (Fig. 3C).

Even though neurons represented the most abundant cell type, we also identified a small population of glial cells. Expression of the astrocytic marker S100B was detectable by 9DIV and reached 5.6 ± 3.5 fold at 49DIV. Expression of GFAP was detected later (21DIV), but showed a similar fold change by 49DIV (4.37 ± 0.86 fold, $p < 0.001$) (Fig. 3D). Immunocytochemistry confirmed the presence of small numbers of morphologically unusual S100β positive glial progenitors with small cell bodies, and long processes amongst the growing neuronal populations (Fig. 2J). The oligodendrocyte progenitor marker OLIG2, also did not change significantly during the experiment, but appeared to show a small burst of expression at 14DIV and 21DIV (Fig. 3D).

3.3. Characterization of neurochemical and morphological phenotypes by ICC and qPCR

The metabotropic glutamate receptors (subtype 2-GRM2 and subtype 5-GRM5), which are activated through second messenger pathways, showed a significant increase in expression during the differentiation. Expression of GRM5 gradually increased from the 14-day NS stage, and reached a peak expression of 41.37 ± 6 fold at 49DIV ($p < 0.001$). Expression of GRM2 plateaued briefly at 14DIV (24.4 ± 2.7 fold) before continuing to increase to 74.25 ± 19 fold at 49DIV ($p < 0.01$) (Fig. 4A).

NMDA receptor 1 (NR1) plays a critical role in regulating Ca^{2+} influx during glutamatergic transmission through ionotropic channels. Expression of NR1 increased from 14DIV to 21DIV (31.83 ± 4 fold, $p < 0.01$), and continued to rise until 49DIV (39 ± 5.87 fold, $p < 0.001$). Expression of DLG4, encoding the protein postsynaptic density 95 (PSD-95), which is an essential component in regulating glutamate release and re-uptake during the interaction with NMDA receptors, increased less dramatically, rising only 3.8 ± 1.1 fold ($p < 0.01$) at 49DIV (Fig. 4B).

Expression of markers for inhibitory GABAergic neurons, on the other hand, showed a much later maturation but greater fold changes. Neurons in our culture expressed genes for two of the most important GABA synthetic enzymes, namely GAD67 (encoded by GAD1) and GAD65 (encoded by GAD2). Their expression increased 70 ± 19 fold ($p < 0.01$) and 99 ± 12 fold ($p < 0.001$), respectively, at 49DIV while the GABA receptor1 (GABBR1) increased 111 ± 51 fold ($p < 0.05$) by 49DIV (Fig. 4C).

We also detected two enzymes involved in cholinergic neurotransmission, CHAT and ACHE, however with much lower increases in expression as compared to the GABAergic or glutamatergic markers. Expression of CHAT showed a small increase of expression at 14DIV (2.12 ± 0.37 fold, $p < 0.05$) and 21DIV (1.77 ± 0.15, $p < 0.05$) before declining by 49DIV. Expression of ACHE peaked by 21DIV and remained elevated at 49DIV (3.87 ± 0.72 fold, $p < 0.01$). Expression of TH, an enzyme required for dopaminergic synthesis, showed elevated expression at 21DIV (2.3 ± 0.39 fold, $p < 0.01$), and continued to rise until 49DIV (6.2 ± 0.6 fold, $p < 0.001$) (Fig. 4D).

ICC staining confirmed the gene expression data showing that staining of NR1 was largely confined to cell bodies, often with typical pyramidal morphologies (Fig. 4E, white arrow). PSD-95 staining was

punctate with nodes distributed along dendrites stained with MAP2 (Fig. 4F, white arrow). VGluT1, which transports glutamate from the cytoplasm to synaptic vesicles, stained strongly in the cytoplasm of many 49DIV neurons (Fig. 4G, white arrow). Staining of GAD67 was extensively expressed in our 49DIV culture, and associated with both the cell body and processes (Fig. 4H, white arrow).

4. Discussion

In this study, we describe the establishment of a novel, long-term culture method that was developed by adapting two of the more commonly described differentiation methods, the classic NS attachment (Dottori and Pera, 2007) and the dissociation methods (Zhang and Zhang, 2010). This new culture method allows for a long-term (over 7 weeks) culture of healthy neurochemically and structurally mature neurons.

We postulated that performing dissociation when the NSs were 28 days old would minimise damage to the early progenitors, which are reported to still need strong cell-cell contact for survival (Svendsen et al., 1998). During the adhesion phase of our combined method, neural progenitors within the NSs and those that migrated out of the NSs were allowed to further proliferate, rather than push towards differentiation. Thus, at 28DIV of the adhesion phase, approximately 50% of the cells in the un-dissociated culture retained an immature neural progenitor phenotype (Fig. 2B, C). After dissociation at 28DIV, the cells recovered for approximately 7 days and by 39DIV, the Nestin positive progenitor phenotype had nearly disappeared (10%, Fig. 2L). By contrast, a more mature MAP2 and NeuN positive population emerged (Fig. 2, D, G, L), and this continued until complex structure in cultures had evolved at 50DIV (Fig. 2, F, I, L). By dissociating cells half way through the “classic” period of NS culture, the benefits of continued progenitor amplification and slow differentiation have been captured before the detachment and death take place. These cells respond better to dissociation than if this occurs very early in the NS growth (14-day NSs) stage, and thus are able to grow and differentiate successfully. This model does not have the problem of cell detachment, and we were able to maintain cultures in good health for at least 21 further days after dissociation, and successfully established consistently uniform cultures of neurons that are amenable to morphological characterisation.

Culture of small NS clusters for longer than 7 weeks was reported in only a few studies (Itsykson et al., 2005; Yla-Outinen et al., 2014; Lappalainen et al., 2010b), however, these studies lacked detailed cell lineage analysis, especially the neuronal transmitter characterisation as described here. For examples, Itsykson et al only reported the expression of βIII-tubulin as the marker for neurons while Lappalainen et al utilized βIII-tubulin and MAP2 as the markers for neurons. More importantly, most of the current studies adopted the method of seeding whole NSs in the culture, which created a very heterogeneous cell distribution that was difficult to analyse (Itsykson et al., 2005; Erceg et al., 2008).

After the neural culture was established, we performed detailed characterisation to be able to understand the temporal profile of the neural differentiation in our culture system. We found that expression of the stem cell markers NESTIN, SOX2 and PAX6 did not change significantly during the experiments (Fig. 3A, B). This suggests that once the NSs were plated down, they shifted from stem cell proliferation to neural progenitor proliferation and differentiation, consistent with the morphological maturation with extensive axon and dendrite sprouting.

Our results also suggest that active axonal outgrowth began at 9DIV as indicated by the expression of the growth cone marker GAP43 (Fig. 3C). Expression of the synaptic protein Synapsin-1 steadily increased in expression every 7 days (Fig. 3C). By 49DIV, gene expression of Synapsin-1 reached its maximum, and ICC revealed extensive positive punctate structures believed to be synapses (Fig. 2I). These findings indicate a high level of neuronal maturation.

Since electrophysiology was not available for this experiment, to better understand the neurochemical phenotype of our cultures, we assessed the level of expression and distribution of a range of different neuron transmitters by qPCR and ICC.

Gene expression of two glutamatergic receptors, ionotropic (NR1) and metabotropic (mGluR2, mGluR5) was upregulated markedly once the differentiation was initiated, and surged to 39, 74, and 41-fold, respectively at 49DIV compared to 14-day NSs. ICC for NR1 showed wide spread distribution of NMDA receptors in the 49DIV neurons possessing typical pyramidal morphologies (Fig. 4E). This is important because range of studies suggest that 70-80% of the total neurons in the cortex are pyramidal glutamatergic neurons (as reviewed in Markram et al., 2004).

Conversely, we did not see as dramatic a change in expression of DLG4, the gene for PSD-95. However, this essential component of excitatory neurotransmission was readily detected in punctate structures along the MAP2 positive processes (Fig. 4F) by ICC at 49DIV. VGluT1 also had extensive expression in 49DIV neurons, with the protein detected not only in the pyramidal neurons cell bodies, but also along their processes, consistent with the previous study reporting increasing VGluT1 expression in glutamatergic neuron synapses that are ensheathed by processes from individual developing astroglia *in vivo* (Morel et al., 2014). These results indicate rapid maturation of two major glutamate receptor types in large numbers of glutamatergic neurons in our cultures.

GABA synthesis requires the activation of glutamate decarboxylase genes (GAD1 and GAD2), which in our cultures showed a 30-fold increase at 21DIV, and a 99- and 70-fold increase at 49DIV, respectively. GABBR1, which is mainly located post-synaptically, had an even higher expression of 111-fold compared to 14-day NSs. The GABAergic neurons showed various morphologies, appearing as both pyramidal and bipolar, which were consistent with similar features previously found in cortical interneuron populations (Markram et al., 2004).

Conversely, we found that expression of the cholinergic genes for ChAT and ACHE only increased 2-fold and 4-fold, respectively at 49DIV. This suggests that our culture method does not lead to a population of neurons typical of cortical layers II-III where small bipolar cholinergic neurons predominately reside (von Engelhardt et al., 2007).

Similarly, under spontaneous neural induction conditions in our cultures, expression of TH only showed a 6-fold increase at 49DIV, suggesting that the cultures lack signals like fibroblast growth factor 8 (FGF8) and sonic hedgehog (SHH) required to stimulate differentiation of forebrain dopaminergic neuronal populations (Hynes and Rosenthal, 1999).

We also detected only low levels of glial marker expression for astrocytes and oligodendroglial progenitors. This makes these cultures suitable for the study of the influence of adding these cells in different proportions and times during the culture maturation.

This is the first description of generation of a neural population with mixed forebrain neurotransmitter characteristics. In the future, the addition of supplementary patterning factors could be used to further enriched the cultures for specific neuronal types.

The limitation of our study is lacking electrophysiological characterisation. However, other have shown that expression of the pan-neuronal markers β-III tubulin usually appears at the same stage as the ability to generate action potentials while the expression of specific neuronal marker such as GAD1 is associated with spontaneous electrical activity (Belinsky et al., 2014). Another limitation of our methods is that the current manual cutting method limits scalability for high-through-put studies.

Taken together, we have established a simple and reproducible method to generate structurally mature neuronal populations from hESCs. The molecular markers of neurochemical specificity (synthetic enzymes), structural maturity (axons, synapses, post-synaptic densities) and functional maturity (neurotransmitter receptors and transporters) show increased expression after 21DIV and have increased further by 49DIV. ICC confirms that proteins such as NR1, PSD-95, VGluT1 and

GAD1 which are required to sub-serve electrical activity are also present at 49DIV.

5. Conclusion

We have described a new *in vitro* method for the generation of clinically relevant human neurons from hESCs. These neurons are morphologically and neurochemically mature. We believe these cultures will provide a useful tool for the study of human neurological diseases and drugs used to treat them.

Conflict of interest

The authors declare that they have no conflict of interest.

Acknowledgments

This work was supported by fund from “Biomarkers for assessing effectiveness of hypothermia as a therapy in ischaemic stroke” (grant number: 1037863).

Appendix A. Supplementary data

Supplementary material related to this article can be found, in the online version, at doi:https://doi.org/10.1016/j.jneumeth.2018.07.005.

References

Hazzouri, Zeki Al, A, MN Haan, Deng, Y., Neuhaus, J., Yaffe, K., 2014. Reduced heart rate variability is associated with worse cognitive performance in elderly Mexican Americans. Hypertension 63, 181–187.

Alheim, K., Bartfai, T., 1998. The interleukin-1 system: Receptors, ligands, and ICE in the brain and their involvement in the fever response. In: McCann, S.M., Lipton, J.M., Sternberg, E.M., Chrousos, G.P., Gold, P.W., Smith, C.C. (Eds.), Neuroimmunomodulation: Molecular Aspects, Integrative Systems, and Clinical Advances, pp. 51–58.

Landis, S.C., Amara, S.G., Asadullah, K., Austin, C.P., Blumenstein, R., Bradley, E.W., Crystal, R.G., Darnell, R.B., Ferrante, R.J., Fillit, H., Finkelstein, R., Fisher, M., Gendelman, H.E., Golub, R.M., Goudreau, J.L., Gross, R.A., Gubitz, A.K., Hesterlee, S.E., Howells, D.W., Huguenard, J., Kelner, K., Koroshetz, W., Krainc, D., Lazic, S.E., Levine, M.S., Macleod, M.R., McCall, J.M., Moxley 3rd, R.T., Narasimhan, K., Noble, L.J., Perrin, S., Porter, J.D., Steward, O., Unger, E., Utz, U., Silberberg, S.D., 2012. A call for transparent reporting to optimize the predictive value of preclinical research. Nature 490, 187–191.

Thomson, J.A., Itskovitz-Eldor, J., Shapiro, S.S., Waknitz, M.A., Swiergiel, J.J., Marshall, V.S., Jones, J.M., 1998. Embryonic stem cell lines derived from human blastocysts. Science 282, 1145–1147.

Carpenter, M.K., Inokuma, M.S., Denham, J., Mujtaba, T., Chiu, C.P., Rao, M.S., 2001. Enrichment of neurons and neural precursors from human embryonic stem cells. Exp Neurol 172, 383–397.

Reubinoff, B.E., Itsykson, P., Turetsky, T., Pera, M.F., Reinhartz, E., Itzik, A., Ben-Hur, T., 2001. Neural progenitors from human embryonic stem cells. Nat Biotechnol 19, 1134–1140.

Dhara, S.K., Hasneen, K., Machacek, D.W., Boyd, N.L., Rao, R.R., Stice, S.L., 2008. Human neural progenitor cells derived from embryonic stem cells in feeder-free cultures. Differentiation 76, 454–464.

Prajumwongs, P., Weeranantanapan, O., Jaroonwitchawan, T., Noisa, P., 2016. Human Embryonic Stem Cells: A Model for the Study of Neural Development and Neurological Diseases. Stem Cells Int 2016, 2958210.

Shinde, V., Sureshkumar, P., Sotiriadou, I., Hescheler, J., Sachinidis, A., 2016. Human Embryonic and Induced Pluripotent Stem Cell Based Toxicity Testing Models: Future Applications in New Drug Discovery. Curr Med Chem 23, 3495–3509.

Datta, I., Ganapathy, K., Tattikota, S.M., Bhonde, R., 2013. Directed differentiation of human embryonic stem cell-line HUES9 to dopaminergic neurons in a serum-free defined culture niche. Cell Biology International 37, 54–64.

Lee, N., Choi, C., Jeon, I., Song, J., 2009. Differentiation of GABAergic Neurons from Human Embryonic Stem Cells. Tissue Engineering and Regenerative Medicine 6, 1359–1365.

Chambers, S.M., Fasano, C.A., Papapetrou, E.P., Tomishima, M., Sadelain, M., Studer, L., 2009. Highly efficient neural conversion of human ES and iPS cells by dual inhibition of SMAD signaling. Nat Biotechnol 27, 275–280.

Lappalainen, R.S., Salomaki, M., Yla-Outinen, L., Heikkila, T.J., Hyttinen, J.A.K., Pihlajamaki, H., Suuronen, R., Skottman, H., Narkilahti, S., 2010a. Similarly derived and cultured hESC lines show variation in their developmental potential towards neuronal cells in long-term culture. Regenerative Medicine 5, 749–762.

Axell, M.Z., Zlateva, S., Curtis, M., 2009. A method for rapid derivation and propagation of neural progenitors from human embryonic stem cells. J Neurosci Methods 184, 275–284.

Pasca, A.M., Sloan, S.A., Clarke, L.E., Tian, Y., Makinson, C.D., Huber, N., Kim, C.H., Park, J.Y., O’Rourke, N.A., Nguyen, K.D., Smith, S.J., Huguenard, J.R., Geschwind, D.H., Barres, B.A., Pasca, S.P., 2015. Functional cortical neurons and astrocytes from human pluripotent stem cells in 3D culture. Nat Methods 12, 671–678.

Dottori, Pera, M.F., 2007. Neural differentiation of human embryonic stem cells. Methods Mol Biol 438, 19–30.

Schmittgen, T.D., Livak, K.J., 2008. Analyzing real-time PCR data by the comparative C(T) method. Nat Protoc 3, 1101–1108.

Zhang, X.Q., Zhang, S.C., 2010. Differentiation of neural precursors and dopaminergic neurons from human embryonic stem cells. Methods Mol Biol 584, 355–366.

Svendsen, C.N.M.G., Borg, ter, Richard, J.E., 1998. A new method for the rapid and long term growth of human neural precursor cells. Journal of neuroscience methods 141–152.

Itsykson, P., Ilouz, N., Turetsky, T., Goldstein, R.S., Pera, M.F., Fishbein, I., Segal, M., Reubinoff, B.E., 2005. Derivation of neural precursors from human embryonic stem cells in the presence of noggin. Molecular and Cellular Neuroscience 30, 24–36.

Yla-Outinen, L., Joki, T., Varjola, M., Skottman, H., Narkilahti, S., 2014. Three-dimensional growth matrix for human embryonic stem cell-derived neuronal cells. J Tissue Eng Regen Med 8, 186–194.

Lappalainen, R.S., Salomaki, M., Yla-Outinen, L., Heikkila, T.J., Hyttinen, J.A., Pihlajamaki, H., Suuronen, R., Skottman, H., Narkilahti, S., 2010b. Similarly derived and cultured hESC lines show variation in their developmental potential towards neuronal cells in long-term culture. Regen Med 5, 749–762.

Erceg, S., Lainez, S., Ronaghi, M., Stojkovic, P., Perez-Arago, M.A., Moreno-Manzano, V., Moreno-Palanques, R., Planells-Cases, R., Stojkovic, M., 2008. Differentiation of human embryonic stem cells to regional specific neural precursors in chemically defined medium conditions. PLoS One 3, e2122.

Markram, H., Toledo-Rodriguez, M., Wang, Y., Gupta, A., Silberberg, G., Wu, C., 2004. Interneurons of the neocortical inhibitory system. Nat Rev Neurosci 5, 793–807.

Morel, L., Higashimori, H., Tolman, M., Yang, Y., 2014. VGluT1 + neuronal glutamatergic signaling regulates postnatal developmental maturation of cortical protoplasmic astroglia. J Neurosci 34, 10950–10962.

von Engelhardt, J., Eliava, M., Meyer, A.H., Rozov, A., Monyer, H., 2007. Functional characterization of intrinsic cholinergic interneurons in the cortex. J Neurosci 27, 5633–5642.

Hynes, M., Rosenthal, A., 1999. Specification of dopaminergic and serotonergic neurons in the vertebrate CNS. Curr Opin Neurobiol 9, 26–36.

Belinsky, G.S., Rich, M.T., Sirois, C.L., Short, S.M., Pedrosa, E., Lachman, H.M., Antic, S.D., 2014. Patch-clamp recordings and calcium imaging followed by single-cell PCR reveal the developmental profile of 13 genes in iPSC-derived human neurons. Stem Cell Res 12, 101–118.